EFDA–JET–PR(12)09

L. Snoj, A. Trkov, I. Lengar, S. Popovichev, S. Conroy, B. Syme
and JET EFDA contributors

Calculations to Support JET Neutron Yield Calibration: Neutron Scattering in Source Holder

Calculations to Support JET Neutron Yield Calibration: Neutron Scattering in Source Holder

L. Snoj[1], A. Trkov[1], I. Lengar[1], S. Popovichev[2], S. Conroy[3], B. Syme[2]
and JET EFDA contributors*

JET-EFDA, Culham Science Centre, OX14 3DB, Abingdon, UK

[1]EURATOM-MHEST Association, Reactor Physics Division, Jožef Stefan Institute, Jamova cesta 39, SI-1000 Ljubljana, Slovenia
[2]EURATOM-CCFE Fusion Association, Culham Science Centre, OX14 3DB, Abingdon, OXON, UK
[3]EURATOM-VR Association, Department of Physics and Astronomy, Uppsala University, Box 516, SE-75120 Uppsala, Sweden
** See annex of F. Romanelli et al, "Overview of JET Results", (23rd IAEA Fusion Energy Conference, Daejon, Republic of Korea (2010)).*

Preprint of Paper to be submitted for publication in
Fusion Engineering and Design

ABSTRACT

After the coated CFC wall to ITER-Like Wall (Beryllium/Tungsten/Carbon) transition in 2010-11, confirmation of the neutron yield calibration will be ensured by direct measurements using a calibrated ^{252}Cf neutron source deployed by the in-vessel remote handling boom and Mascot manipulator inside the JET vacuum vessel.

The paper describes preliminary calculations and the results of numerical study of the effect of source holder on neutron detector response. The source baton was designed in such a way, that it does not significantly affect the neutron spectrum, angular neutron flux distribution or activation detector response. All effects are approximately equal to or less than 1%. The largest disturbance to the neutron flux angular distribution and to the neutron spectrum arises from the source capsule. Hence one should obtain as much information as possible about the capsule and the ^{252}Cf source material in order to avoid additional systematic errors.

1. INTRODUCTION

In 2010-11 the Joint European Torus (JET) plasma facing wall was changed from a Carbon wall to an ITER-Like Wall (Beryllium/Tungsten/Carbon). After that transition, the update of the JET neutron yield calibration will be ensured by direct measurements using a calibrated ^{252}Cf neutron source deployed inside the JET vacuum vessel [1].

This calibration will allow direct confirmation of the calibration of the external fission chambers (which was the standard on JET originally [2]) and provide the first direct calibration of the JET activation system. The fission chamber system consists of sets of fission chambers mounted on three JET transformer limbs, which provide the time-dependent neutron yield used to assess a JET pulse. Activation Detectors (AD) are part of the JET activation neutron monitoring system, which determines the absolute neutron yields and hence the absolute calibration of time-resolved neutron yield monitors. The activation system pneumatically delivers capsules to positions just at the edge of the vacuum-vessel inside JET, where they are irradiated during the pulse, pneumatically retrieved, and the induced activity is measured to provide a time-integrated absolute fusion yield measurement. All these measurement systems will be relevant to the D-D plasma calibrations.

The calibration of the neutron detectors will be performed by moving a standardized ^{252}Cf point neutron source inside around the vacuum vessel and observing the detector response.

The neutron source will be deployed on the JET Mascot robot. In order to safely manipulate the neutron source with the robot, the source will be placed in a specially designed tube (source baton), which will connect to the mascot robot via a longer tube, called the mascot baton. The two batons approach is needed in order to ensure adequate separation of neutron source from the robot body, to reduce neutron scattering from the mascot robot, to reduce activation of the robot and to limit the dose on the robot cameras. The source baton has to be short enough to allow source transport inside it and inside the normal Transport Flask.

The baton is subject to several design constraints; it should be robust, the connection of the

source and mascot baton should be fail-safe and the baton should not significantly disturb the spatial neutron flux distribution and energy spectrum of the neutron source. The latter point is especially important for accurate calibration. Hence a set of neutronic calculations is needed to support the baton design.

The requirement for accuracy in the neutron yield determination is 10%. In order to significantly improve the accuracy of the calibration, a whole set of calculations is required to support the JET neutron calibration project. Many are based on Monte Carlo modelling using the advanced Monte Carlo transport codes, such as MCNP [6].

Several computational analyses to support JET neutron yield calibration have already been performed, such as analyses of contributions to the external neutron monitor responses [3] and modelling of the JET remote handling system [4].

The purpose of this paper is to examine the effect of the baton on angular neutron flux distribution around the source holder, on neutron flux and spectrum and on JET activation detector response. In addition we study the effect of ^{252}Cf spontaneous fission neutron spectrum from various data sources on the activation detector response.

2. NEUTRON SOURCE AND BATON DESIGN

There are several types of Cf neutron sources and their casings that are used for housing the ^{252}Cf. Some of them are described in the QSA Global information sheet [5]. In our calculations we used the X.224 stainless steel capsule. The source dimensions are presented in Figure 1.

The neutron source holder or "baton" consists of the source baton, which contains the neutron source and the mascot baton which connects the source baton to the mascot robot. The baton is presented in Figure 2.

It is important to note that these figures present the preliminary design of the baton, which reflects the status of the design as of July 2010. The final design of the bare source and the baton can and probably will change, but not significantly. Hence the basic finding and conclusions made in this paper can be applied (in a conservative sense) to the actual bare source and baton design as well.

3. CALCULATIONS

3.1 COMPUTATIONAL TOOL

The calculations presented in the report were performed using the MCNP code (version 5.1.40), which is one of the most advanced and verified computer codes for Monte Carlo transport of neutrons and photons. MCNP is a general purpose Monte Carlo transport code used for calculation of detector efficiencies, dose fields, radiological shielding, criticality calculations and nuclear reactor calculations [6]. All calculations were performed with ENDF/B-VI.8 [7] cross section library, which usually comes with the MCNP code package itself. It is important to note that the calculations were separately performed using the FENDL 2.2 [8], JEFF 3.1 [9] and ENDF/B-VII.0 [10] cross section libraries as well, but no statistically significant differences were observed.

The error bars in all figures represent 1s statistical standard uncertainty of the Monte Carlo calculations, unless stated otherwise.

3.2 COMPUTATIONAL MODEL

In the calculations we used SDEF card in MCNP to model the ^{252}Cf spontaneous fission neutron point source. The point source was located in the middle of the source casing void; its position is marked with a cross in Figure 3. If not stated otherwise the source used in our calculation is a point source.

The 252Cf spontaneous fission neutron spectrum was taken from the IRDF-2002 [11], unless stated otherwise. Other neutron spectra are used in the analysis of the effect of neutron spectra on the AD response and the results are presented in section 5.

The MCNP geometrical model was based on the design drawings of the baton and the source. The computational model of the source casing (bare source) is presented in Figure 3 and is based on Figure 1. This type of source (X.224) was used in all calculations. The computational model of the complete source holder consisting of source baton and the mascot baton is presented in Figure 4 and is based on Figure 2. The major axis of the source holder and source casing is along the X axis, from which the angle is measured.

We placed 40 spherical neutron detectors in the azimuthal (XY) and 40 in poloidal (YZ) directions, in order to examine the angular neutron flux distribution as seen in Figure 5. The detectors are spheres (radius = 10cm), centred at 300cm from the point neutron source (located at $X = 0, Y = 0, Z = 0$), in which the neutron flux is tallied using the track length estimator (F4 tally in MCNP). The detectors are void (as everything else around the source) and therefore do not perturb the neutron flux. The detector azimuthal angle is measured from the X axis in XY plane.

In order to examine the total neutron emission and the neutron spectra we surrounded the source holder with a sphere (radius = 100 cm) completely surrounding the source holder (covering the 4π angle). In this case the neutron flux was calculated by using the surface flux estimator (F2 tally in MCNP).

The neutron flux was calculated either by using the track length estimator (F4 tally in MCNP) or the surface flux estimator (F2 tally in MCNP). The neutron spectrum was calculated by tallying neutron flux in energy bins. The activation detector response was calculated by multiplying the neutron flux spectrum by the inelastic scattering cross section for ^{115}In (^{115}In(n,n')^{115m}In) from IRDF-2002 (Figure 6). The latter was done by using the tally multiplier card (FM) in MCNP.

4. RESULTS

4.1 AZIMUTHAL SCAN

The azimuthal scan was performed in order to examine the disturbance of the baton (source baton + mascot baton + bare source inside the source baton) and the source casing (bare source) to the neutron flux. Poloidal scans were investigated to check the computational method and model, but the results are not presented in the graphs, as the neutron flux is confirmed to be isotropic in poloidal

direction because of the axially symmetric structures surrounding the neutron source.

As it is difficult to observe the differences when plotting the neutron flux distributions, we plotted the difference in neutron flux and in activation detector response distributions. The relative difference between the two cases was calculated using the following formula

$$\Delta_{AB,i} = \frac{\varphi_{A,i}}{\varphi_{B,i}} - 1, \tag{1}$$

where $\Delta_{AB,i}$ is the relative difference in i-th detector tally (neutron flux or activation detector response) between case A (bare source, baton, volumetric source) and case B (void, bare source or point source) and $\phi_{A,i}$ is the tally (neutron flux or activation detector response) in i-th detector in case A.

The baton should be designed in such way, that its effect on angular neutron flux is as low as reasonably achievable. We performed a whole suite of calculations to optimize the baton design and finished with 1mm thick Al baton. The process of optimization is out of scope of this paper and therefore not described here. The main purpose of the present paper is to examine the effect of the baton on the angular neutron flux distribution.

The relative differences in neutron flux and activation detector response in azimuthal neutron detectors due to presence of the baton are shown in Figure 7.

It can be observed that the baton only slightly disturbs the angular neutron flux distribution, indicating that the baton design is very good from the neutronic point of view. The neutron flux directly in front of the source casing and the sides is increased by approximately 0.5%, which is due to scattering of neutrons from the casing. Two depressions (–1.5) at ± 25° are a consequence of the "edge effect" as the baton at the edges is effectively thicker and of the scattering of neutrons from the edge to other angles is increased. In the backward direction the attenuation is significant due to relatively long and massive mascot baton and its components. However, in backward direction the JET mascot robot and the boom also affect the neutron flux.

The activation sample response exhibits a similar trend to the neutron flux; with the exception that there is no increase in front and side detectors. This means that the spectrum in that region is slightly "softer", i.e. moved towards lower energies, because of the multiple scatterings on the source baton. The effect is seen as the activation reaction has a threshold at approximately 0.5MeV. This conclusion is confirmed by the neutron spectrum calculation discussed in section 4.2.

In addition we examined the effect of the source casing (bare source) on the azimuthal distribution of the neutron flux and Activation Detector (AD) response in comparison with a "perfect" virtual point source in empty space (void). The results are presented in Figure 8 left. The void case was examined in order to demonstrate the size of the effect the source casing has on the azimuthal distribution and to allow estimation of the potential effects of the source casing on the results.

Of course the neutron source casing significantly disturbs the angular neutron flux distribution. The neutron flux directly in front of the source casing and the sides is increased by approximately 2%, which is due to scattering of neutrons from the casing. Two large depressions at ±20° are a

consequence of the "edge effect" as the source casing at the edges is effectively thicker and of the scattering of neutrons from the edge to other angles, where neutron flux is increased. There is a strong attenuation of neutron flux due to source casing in the backward direction due to the relatively thick pin of the X.224 source casing. Again it is important to note that these changes in angular neutron flux are unavoidable for this source casing design.

The activation sample response exhibits a similar trend to the neutron flux; with the exception that there is no increase in side detectors. This means that the spectrum in that region is slightly "softer", i.e. moved towards lower energies, because of the multiple scatterings on source casing and the source baton.

All calculations described above were performed by using the point source model. As the real neutron source is a volumetric source, either a Cf wire or Cf dispersed in ceramics, we performed the same calculations with a volumetric source as well. In our case the neutrons were emitted uniformly from the space inside the neutron casing (the uncoloured region inside the source casing in Figure 3), which was in this case filled with ceramics, Al2O3 or so called alundum. The results for neutron flux and activation detector response are presented in Figure 8 (right). It can be observed that the neutron flux and the activation detector response are both strongly depressed in the front and in the backward direction, mainly due to oblong shape of the source and the corresponding neutron flux attenuation in these directions. At the sides, however, the neutron flux is increased by approximately 2-3%, due to scattering of neutrons from the ceramics. The activation detector response in the side direction remains practically unchanged due to the softer neutron spectrum in that direction. It can be concluded that the ceramic volumetric source affects the neutron flux distribution in two ways: on one hand it scatters neutrons and increases flux in the side direction but changes the neutron spectrum, on the other hand it attenuates the neutron flux in front and back direction. The prevailing effect in certain directions strongly depends on the shape of the volumetric source. As the final source used in calibrations will be much shorter than the one discussed above, the neutron flux attenuation in the forward direction will be smaller.

4.2 NEUTRON SPECTRUM

It was observed that azimuthal distribution of the activation detector response significantly differs from the azimuthal distribution of the neutron flux response due to changes in neutron spectrum. Hence we examined the changes of the neutron spectrum due to the baton and the bare source. The results are presented in Figure 9.

The main change in neutron spectrum occurs due to scattering and slowing down of neutrons on the baton. The neutron flux decreases in the area above 2MeV and increases in the range below 2MeV. Similar conclusions can be made for activation detector response but the differences in the region below 2MeV are slightly larger. The effect of source casing on the neutron flux is similar in shape but different in magnitude, i.e. the effect of source casing (bare source) on the neutron spectrum is approximately twice as big as the effect of the baton. That is mainly due to larger

thickness (1.7mm instead of 1 mm) and different material (Stainless Steel instead of Al).

The measured quantity during the calibration will be the activation of an In disc, which is an integral quantity. Therefore we examined the differences in total neutron flux and total activation detector response (sum over all energies) due to the baton in the 4π solid angle. The results are presented in Table 1. We can observe that the total neutron flux is affected neither by the source casing nor by the baton.

The source casing has the largest effect on the neutron spectrum. The baton, however only slightly perturbs the neutron spectrum (by less than 1%), indicating that the baton design is very good from the neutronics point of view. The total activation detector response, however, is reduced by 1.6% due to baton and bare source, but the majority of the effect (1.2%) comes from the bare source itself, which is practically unavoidable.

5. ^{252}CF SPECTRUM

In addition to the analyses above we performed an analysis of the ^{252}Cf spontaneous fission neutron spectrum from various data sources on the activation detector response. When modelling or defining the ^{252}Cf spontaneous fission neutron spectrum it is very common to use one of the two very widely used approximations, i.e. the Watt fission spectrum approximation defined as:

$$\chi(E) = C\exp\left(\frac{E}{a}\right)\sinh\left(\sqrt{bE}\right)$$
$$E = \text{neutron energy}$$
$$\chi(E) = \text{neutron spectrum} \qquad (1)$$
$$a, b = \text{parameters}$$
$$C = \text{normalisation constant}$$

or the Maxwellian one:

$$\chi(E) = C\sqrt{E}\exp\left(\frac{E}{a}\right)$$
$$E = \text{neutron energy}$$
$$\chi(E) = \text{neutron spectrum} \qquad (2)$$
$$a = \text{parameter}$$
$$C = \text{normalisation constant}$$

The most rigorous approach, however, is to use the evaluated neutron spectrum (e.g. from IRDF-2002 nuclear data file [11]) or the spectrum calculated by using sophisticated nuclear models, e.g. Madland-Nix model [13]. An overview of the above mentioned spectra is presented in Table 2.

All of the above mentioned neutron spectra are depicted in Figure 10a. The ratio between the Watt, Maxwellian, Madland Nix spectra and the IRDF-2002 spontaneous fission neutron spectrum are presented in Figure 10c. It can be observed that the differences between the IRDF-2002 and the Madland-Nix neutron spectra are relatively low, i.e. less than 5% up to 10MeV. The Maxwellian

fission spectrum approximation, however, significantly differs from the IRDF-2002 spectrum already at energies above 5MeV. The Watt fission spectrum approximation differs from the IRDF-2002 at practically all energies.

In our study we are interested in the effect of the choice of ^{252}Cf spontaneous fission neutron spectrum on the activation detector response, i.e. on the ^{115}In(n,n')^{115m}In reaction rate. The differences in the total AD response (sum over all energies) due to different neutron fission spectra are presented in Table 3. By far the largest difference (more than 7 %) is between activation in Watt and IRDF-2002 fission spectra. This is mainly due to relatively higher watt fission spectrum at energies above 2.5MeV. The ^{115}In(n,n')^{115m}In reaction rate spectra in various fission spectra and their differences are presented in Figure 10b and d.

It can be concluded that when calculating reaction rates for threshold reactions such as ^{115}In(n,n')^{115m}In, the shape of neutron spectrum is very important. Hence one should avoid using approximations such as Watt approximations as they might lead to systematic error in the calculated reaction rates. The best option is to use the evaluated neutron spectrum, e.g. from IRDF-2002 nuclear data file, or the spectrum calculated by using sophisticated nuclear models, e.g. Madland-Nix model.

CONCLUSIONS

The paper presents a thorough analysis of the effect of source casing and the baton on neutron monitor response and can serve as a guideline on how to perform such analyses. It is important to note that all the calculations described above are preliminary. The final calibration correction factors should be calculated by modelling the surroundings e.g. vacuum vessel and other tokamak components, JET mascot robot etc., as they might slightly change the effects. It is very likely that the approach with vacuum boundary conditions that we used overestimates the magnitude of the effects as there is no back scattering. Be that as it may, the main conclusions stay the same. The source baton was designed in such way that it does not significantly affect either the neutron spectrum or the activation sample response. Both effects are less than 1%. The largest disturbance to azimuthal neutron flux distribution and to neutron spectrum arises from the source capsule. Hence one should obtain as much information about it and the ^{252}Cf source material as possible in order to avoid additional systematic errors.

It is important to note that the use of the Maxwellian or the Watt fission spectrum approximation is not recommended as it may cause large biases in calculations. Differences of approximately 7% were observed in activation system responses between the Watt and the IRDF-2002 spontaneous fission neutron spectra.

ACKNOWLEDGMENTS

This work was supported by EURATOM and carried out within the framework of the European Fusion Development Agreement. The views and opinions expressed herein do not necessarily reflect those of the European Commission.

REFERENCES

[1]. Syme D.B. et al., Fusion Yield Measurements on JET and their Calibration, Nuclear Engineering and Design, article in press, DOI: http://dx.doi.org/10.1016/j.nucengdes.2011.08.003

[2]. Laundy B.J., Jarvis O. N., Numerical study of the calibration factors for the neutron counters in use at the Joint European Torus, , Fusion technology, vol.24, pages 150-160, September 1993.

[3]. Snoj L. et al., Calculations to support JET neutron yield calibration: contributions to the external neutron monitor responses, Nuclear Engineering and Design, article in press, doi:10.1016/j.nucengdes.2011.07.011

[4]. Snoj L. et al., Calculations to support JET neutron yield calibration: modelling of the JET remote handling system, Proc. Int. Conf. Nuclear Energy for New Europe 2011, Bovec, Slovenia, September, Nuclear Society of Slovenia, 2011,

[5]. Sources, H.T. Californium-252 Spontaneous Fission Neutron Sources. 2010 [cited 2010 24th May]; Infosheet on Cf-252 calibration source]. Available from: http://www.hightechsource.co.uk/generalapplications.html

[6]. X-5 Monte Carlo Team, MCNP - A general Monte Carlo N-particle Transport code, Version 5. 2003(LA-UR-03-1987).

[7]. Victoria McLane, ENDF-201, ENDF/B-VI Summary documentation a supplement I. 1996, National nuclear data center Brookhaven national laboratory: Brookhaven. p.304.

[8]. D. Lopez Aldama, A.T., FENDL-2.1 Update of an evaluated nuclear data library for fusion applications. 2004, International Atomic Energy Agency: Vienna. p.34.

[9]. Koning A., F.R., Kellett M., Mills R., Henriksson H., Rugama Y., The JEFF-3.1 Nuclear Data Library. 2006, Nuclear Energy Agency Organisation for Economic Co-operation and Development: Paris. p.130.

[10]. Chadwick, M.B., et al., ENDF/B-VII.0: Next Generation Evaluated Nuclear Data Library for Nuclear Science and Technology. Nuclear Data Sheets, 2006. **107**(12): p. 2931-3060.

[11]. IAEA, International Reactor Dosimetry file 2002 (IRDF-2002), in Technical report series. 2006, International Atomic Energy Agency: Vienna. p.162.

[12]. J.A. Grundl, V.S., C.M. Eisenhauer, H.T. Heaton, D. M. Gilliam, J. Bigelow, A Californium-252 Fission Spectrum Irradiation Facility for Neutron Reaction Rate Measurements. Nuclear Technology, 1977. **32**: p.315.

[13]. Madland, D.G. and J.R. Nix, Prompt fission neutron spectra and average prompt neutron multiplicities. 1983. Medium: ED; Size: Pages: 36.

	$\frac{\text{baton}}{\text{bare source}}-1$	$\frac{\text{bare source}}{\text{void}}-1$
neutron flux	0.0000	-0.0003
activation detector response	-0.0037	-0.0124

Table 1: Differences in total neutron flux and activation sample response (sum over all energies) due to source baton in comparison with the source casing (bare source): over a 4π solid angle. The statistical uncertainty of the results is less than 0.0001.

Spectrum name	Description	Parameters	Reference
Watt	Watt fission spectrum	a = 1.025 MeV b = 2.926 MeV^{-1}	[6]
Maxwell	Maxwell fission spectrum	a = 1.42 MeV	[7]
IRDF-2002	Evaluated spectrum		[11]
Madland-Nix	Calculated spectrum Madland-Nix model		[13]

Table 2 : Overview of ^{252}Cf spontaneous fission neutron spectra used in our calculations.

Description	Relative difference (%)
$\frac{\text{Maxwell}}{\text{IRDF-2002}}-1$	-0.88 ± 0.01
$\frac{\text{Watt}}{\text{IRDF-2002}}-1$	-7.25 ± 0.01
$\frac{\text{Madland-Nix}}{\text{IRDF-2002}}-1$	-0.40 ± 0.01

Table 3 : Differences in total AD response (sum over all energies) due to different neutron fission spectra. The statistical uncertainty of the calculation is below 0.01.

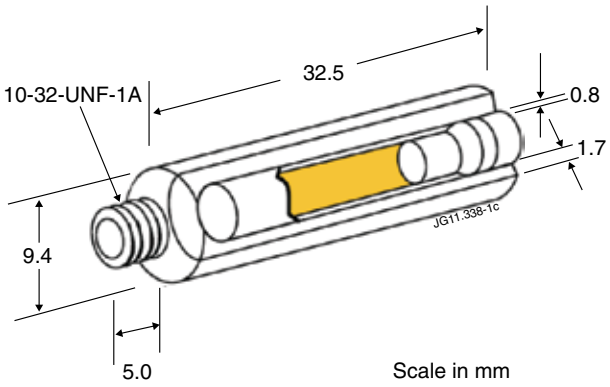

Figure 1: X.224 stainless steel capsule [1].

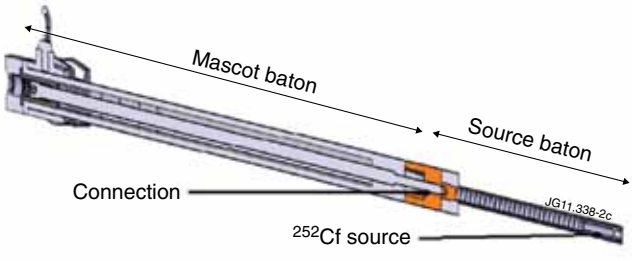

Figure 2: Neutron source holder. Cross sectional view.

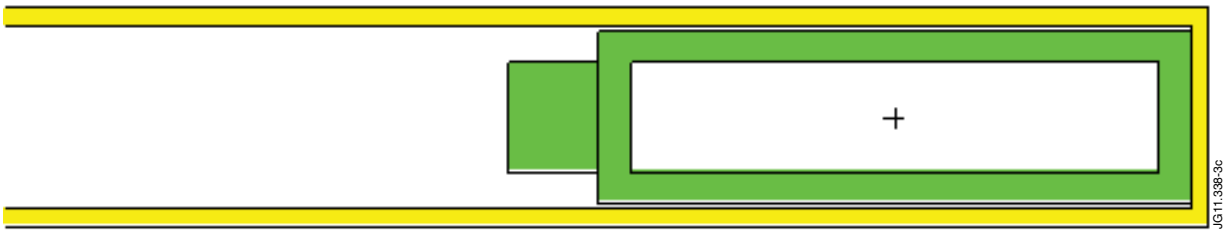

Figure 3: MCNP model of the bare source (green) and the aluminium source baton (yellow). The black cross denotes the position of the modelled point neutron source.

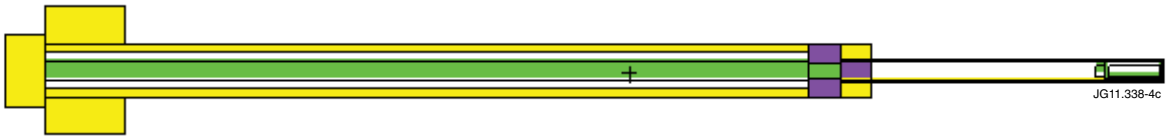

Figure 4: MCNP model of the source holder; stainless steel (green), Aluminium (yellow), Al bronze (purple).

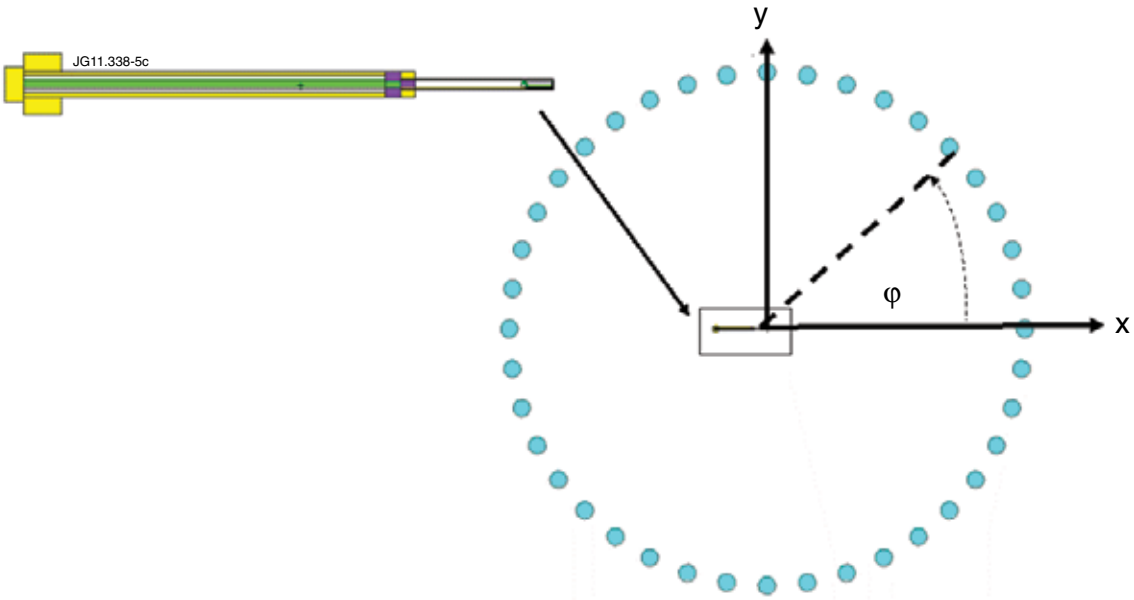

Figure 5: Arrangement of spherical detectors in azimuthal (XY) directions around the neutron source holder.

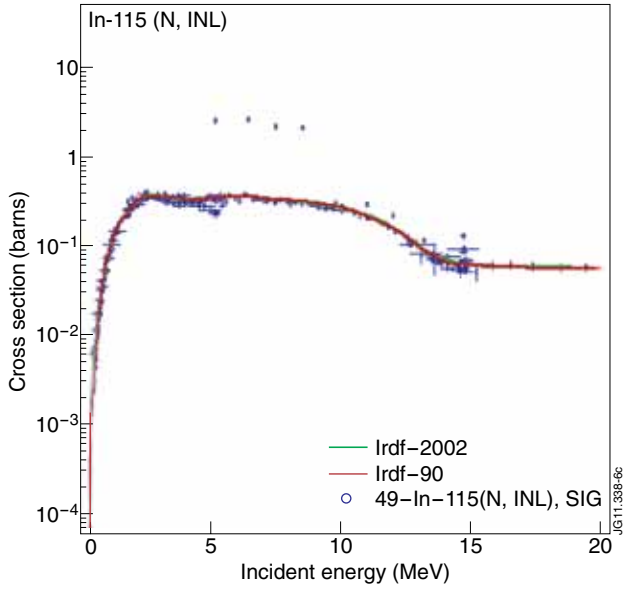

Figure 6: 115In(n,n') 115mIn cross section from IRDF – 2002.

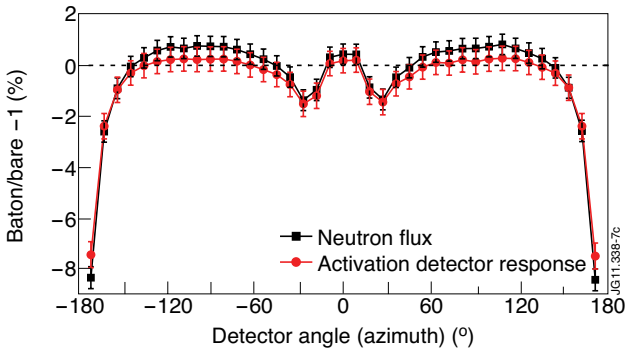

Figure 7: Relative differences in neutron flux and activation detector response in azimuthal neutron detectors due to the baton.

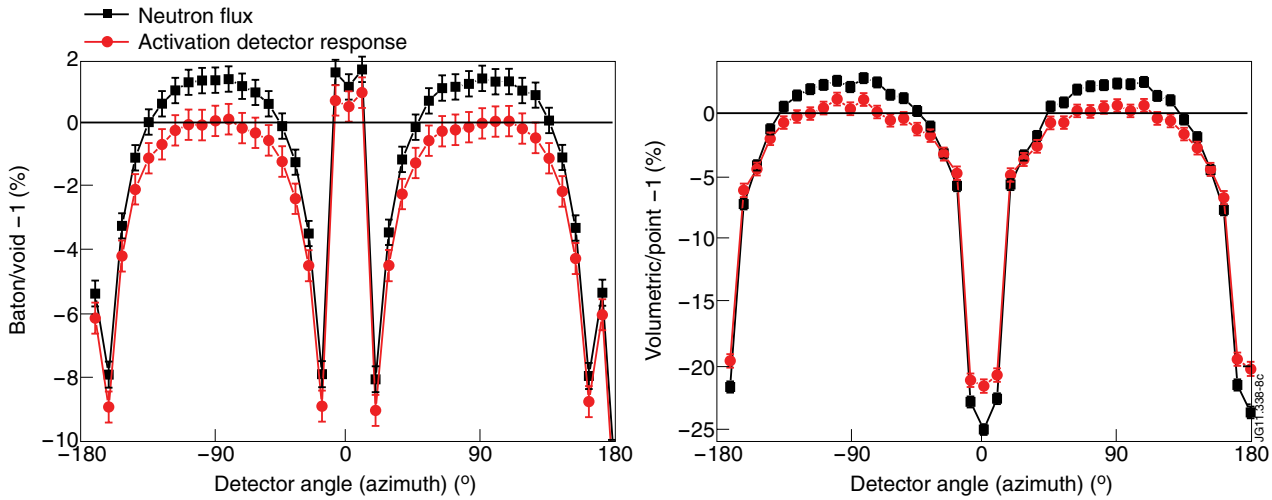

Figure 8: Relative differences in neutron flux and activation detector response in azimuthal neutron detectors due to presence of source casing (left) and volumetric source (right).

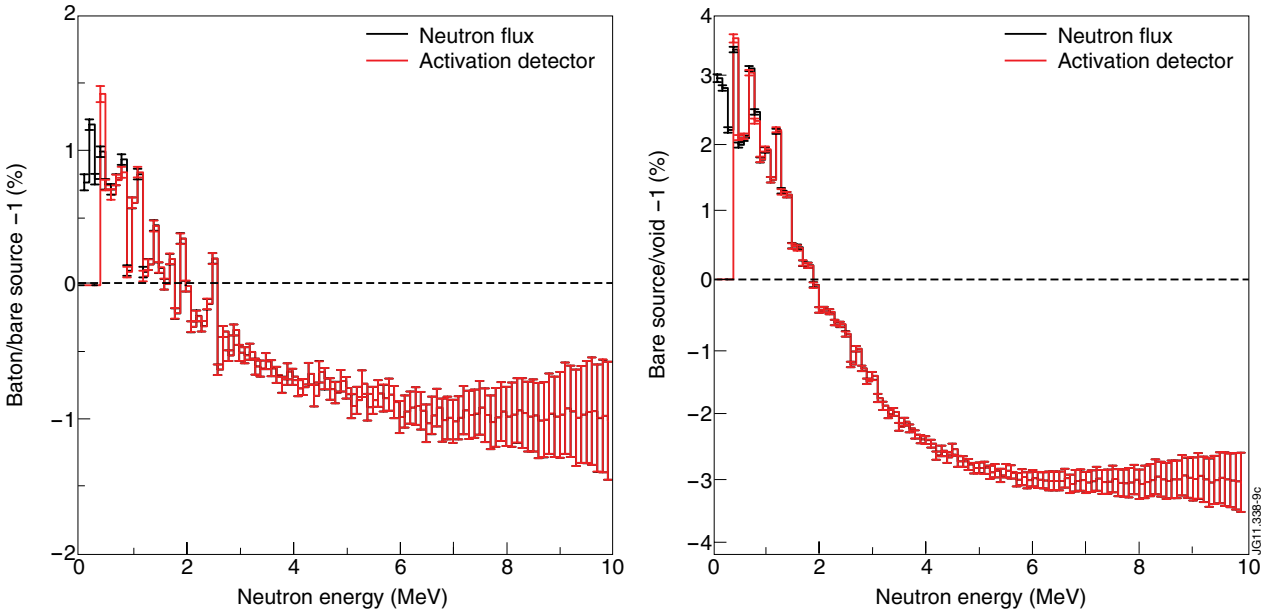

Figure 9: Difference in the neutron flux and the activation detector response due to the baton (left) and the bare source (right) versus neutron energy.

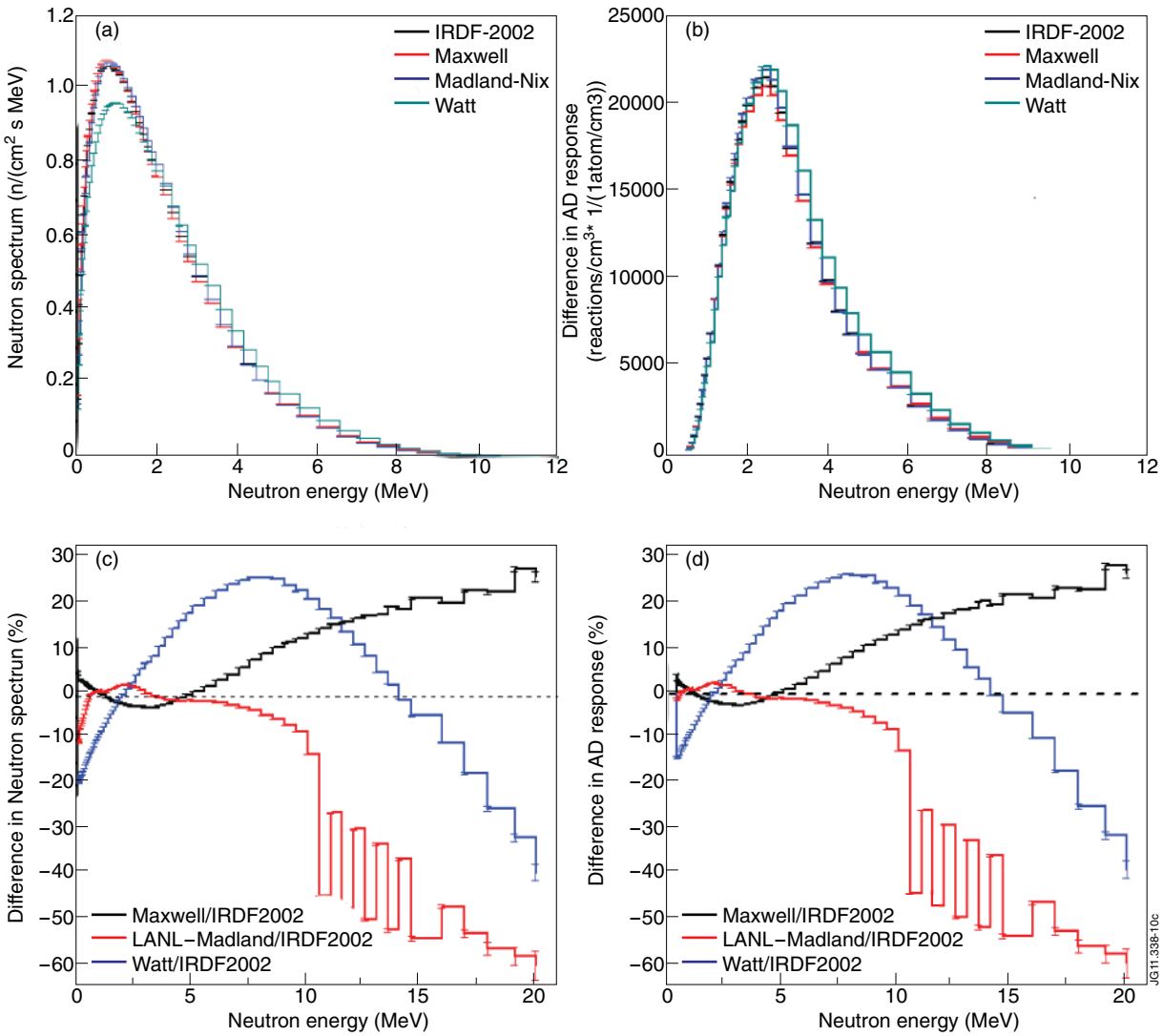

Figure 10: ^{252}Cf spontaneous fission neutron flux spectrum from different sources and the difference in the neutron flux and the activation detector response due to the baton (left) and the bare source (right) versus neutron energy.